

TRANSMISSION POWER VARIANCE CONSTRAINED POWER ALLOCATION FOR ITERATIVE FREQUENCY DOMAIN MULTIUSER SIMO DETECTOR

Valtteri Tervo^{*+}, A Tölli^{*}, J. Karjalainen[†], Tad Matsumoto^{*+}

^{*}Centre for Wireless Communications, University of Oulu, P.O. Box 4500, 90014 University of Oulu, Finland.

⁺Japan Advanced Institute of Science and Technology, 1-1 Asahi-Dai, Nomi, Ishikawa, 923-1292 Japan.

[†]Samsung Electronics R&D Institute UK,

Falcon Business Park, Hali Building, Vaisalantie 4, 01230 Espoo, Finland.

ABSTRACT

Transmission power variance constrained power allocation in single carrier multiuser (MU) single-input multiple-output (SIMO) systems with iterative frequency domain (FD) soft cancellation (SC) minimum mean squared error (MMSE) equalization is considered in this paper. It is known in the literature that peak to average power ratio (PAPR) at the transmitter can be decreased by reducing the variance of the transmit power. In this paper, we derive a power variance constraint to statistically control the PAPR. This constraint is plugged into a convergence constrained power allocation (CCPA) problem and successive convex approximation (SCA) approach via series of geometric programs (GP) is developed. Numerical results are presented in the form of complementary cumulative distribution functions (CCDFs) to demonstrate the effectiveness of the proposed method.

Index Terms— Single carrier, EXIT chart, convergence constraint, geometric program, convex optimization

1. INTRODUCTION

The use of frequency division multiplexing via discrete Fourier transform (DFT) causes a high peak-to-average power ratio (PAPR), which necessitates expensive and power-inefficient radio-frequency (RF) components at the transmitter. Recent work on minimizing the PAPR in single carrier frequency division multiple access (FDMA) [1] transmission can be found in [2–4], where they propose different precoding methods for PAPR reduction. However, these methods do not take into account the transmit power allocation, the channel nor the receiver. PAPR-aware large-scale multiuser (MU) multiple-input multiple-output (MIMO) orthogonal frequency division multiplexing (OFDM) downlink is investigated in [5] where they assume the massive degrees-of-freedom available to achieve low PAPR.

To exploit the full merit of iterative receiver, the convergence properties of an iterative receiver needs to be taken into account at the transmitter side. This issue has been thoroughly investigated in [6] where the power allocation to different channels is optimized subject to a quality of service (QoS) constraint taking into account the convergence properties of iterative frequency domain (FD) soft

cancellation (SC) minimum mean squared error (MMSE) MIMO receiver. The convergence properties were examined by using extrinsic information transfer (EXIT) charts [7]. The concept in [6] has been extended for MU systems in [8, 9]. In this paper, we will introduce a power variance constraint for the convergence constrained power allocation (CCPA) problem presented in [9]. In other words, we will minimize the total transmit power in a cell with multiple users while guaranteeing the desired QoS in terms of bit error probability (BEP) and keeping the transmit power variance always below the desired value. The power allocation presented in this paper requires centralized design, i.e., the base station reports the power allocations to each user. Development towards distributed solution is left as future work.

The main contributions of this paper are summarized as follows: The expected power variance of the transmitted waveform is derived as a function of power allocation. The main reason for controlling the expected power variance is that it is not depending on the transmitted symbol sequence unlike instant PAPR. Hence, a variance constraint is derived and a local convex approximation of the constraint is formulated via geometric program (GP) [10]. The constraint is plugged in to a CCPA problem and solved by successive convex approximation (SCA) algorithm [11].

2. SYSTEM MODEL

Consider a single carrier uplink transmission with U single-antenna users and a base station with N_R antennas as depicted in Fig. 1. Each user's data stream is encoded by forward error correction code (FEC) \mathcal{C}_u , $u = 1, 2, \dots, U$. The encoded bits are bit interleaved and mapped onto a 2^{N_Q} -ary complex symbol, where N_Q denotes the number of bits per modulation symbol. After the modulation, each user's data stream is transformed into the frequency domain by performing the discrete Fourier transform (DFT) and multiplied with its associated power allocation matrix. Finally, before transmission, each user's data stream is transformed into the time domain by the inverse DFT (IDFT) and a cyclic prefix is added to mitigate inter block interference (IBI).

At the receiver side, after the cyclic prefix removal, the signal can be expressed as

$$\mathbf{r} = \mathbf{H}_u \mathbf{F}^{-1} \mathbf{P}_u^{\frac{1}{2}} \mathbf{F} \mathbf{b}^u + \sum_{\substack{y=1 \\ y \neq u}}^U \mathbf{H}_y \mathbf{F}^{-1} \mathbf{P}_y^{\frac{1}{2}} \mathbf{F} \mathbf{b}^y + \mathbf{v}, \quad (1)$$

where $\mathbf{H}_u = [\mathbf{H}_u^1, \mathbf{H}_u^2, \dots, \mathbf{H}_u^{N_R}]^T \in \mathbb{C}^{N_R N_F \times N_F}$ is the space-time channel matrix for user u and $\mathbf{H}_u^r =$

This work was supported by Finnish Funding Agency for Technology and Innovation (TEKES), Academy of Finland, Riitta ja Jorma J. Takanen Foundation, Finnish Foundation for Technology Promotion, Walter Ahlström Foundation, Ulla Tuominen foundation and KAUTE-foundation. This work was also in part supported by the Japanese government funding program, Grant-in-Aid for Scientific Research (B), No. 23360170.

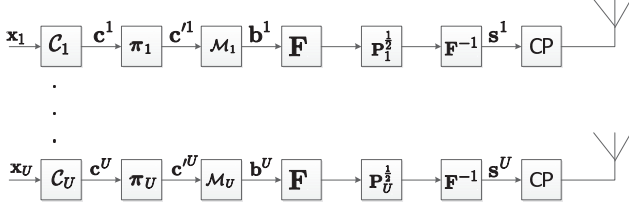


Fig. 1. The block diagram of the transmitter side of the system model.

$\text{circ}\{[h_{u,1}^r, h_{u,2}^r, \dots, h_{u,N_L}^r, \mathbf{0}_{1 \times N_F - N_L}]^T\} \in \mathbb{C}^{N_F \times N_F}$ is the time domain circulant channel matrix for user u at the receive antenna r . The operator $\text{circ}\{\}$ generates matrix that has a circulant structure of its argument vector and N_L denotes the length of the channel impulse response. $\mathbf{F} \in \mathbb{C}^{N_F \times N_F}$ denotes the DFT matrix with elements $f_{m,l} = \frac{1}{\sqrt{N_F}} \exp(i2\pi(m-1)(l-1)/N_F)$. $\mathbf{P} \in \mathbb{R}^{U N_F \times U N_F}$ is the power allocation matrix denoted as $\mathbf{P} = \text{diag}(\mathbf{P}_1, \mathbf{P}_2, \dots, \mathbf{P}_U)$ with $\mathbf{P}_u = \text{diag}(P_{u,1}, P_{u,2}, \dots, P_{u,N_F})^T \in \mathbb{R}^{N_F \times N_F}$, $u = 1, 2, \dots, U$, and $\mathbf{b} = [\mathbf{b}^1, \mathbf{b}^2, \dots, \mathbf{b}^U]^T$. $\mathbf{b}^u \in \mathbb{C}^{N_F}$, $u = 1, 2, \dots, U$, is the modulated complex data vector for the u^{th} user and $\mathbf{v} \in \mathbb{C}^{N_F}$ is white additive independent identically distributed (i.i.d.) Gaussian noise vector with variance σ_v^2 .

3. CONVERGENCE CONSTRAINT

In this section, we will present some of the most important equations related to CCPA. For more details, reader may refer to [6, 8, 9]. The convergence constraint can be expressed as LLR variance constraint as [6, 8, 9]

$$\hat{\sigma}_{u,k}^2 \geq \bar{\sigma}_{u,k}^2, \forall u = 1, 2, \dots, U, \forall k = 1, 2, \dots, K. \quad (2)$$

where $\hat{\sigma}_{u,k}^2$ and $\bar{\sigma}_{u,k}^2$ is the variance of the LLRs at the output of the equalizer and at the input of the decoder, respectively, for u^{th} user at the k^{th} sample point in the EXIT chart. $\bar{\sigma}_{u,k}^2$ is obtained through *diagonal sampling* [9]. When Gray-mapped quadrature phase shift keying (QPSK) modulation is used, the variance of the LLRs at the output of the equalizer can be expressed as [6, Eq. (17)]

$$\hat{\sigma}_{u,k}^2 = \frac{4\zeta_{u,k}}{1 - \zeta_{u,k}\bar{\Delta}_{u,k}}, \quad (3)$$

where $\zeta_{u,k}$ in (3) is called as the effective SINR of the prior symbol estimates and is given by [9]

$$\zeta_{u,k} = \frac{1}{N_F} \sum_{m=1}^{N_F} \frac{P_{u,m} |\boldsymbol{\omega}_{u,m}^k \boldsymbol{\gamma}_{u,m}^H|^2}{\sum_{l=1}^U P_{l,m} |\boldsymbol{\omega}_{l,m}^k \boldsymbol{\gamma}_{l,m}^H|^2 \bar{\Delta}_{u,k} + \|\boldsymbol{\omega}_{u,m}^k\|^2 \sigma_v^2}, \quad (4)$$

where $\boldsymbol{\gamma}_{u,m} \in \mathbb{C}^{N_R}$ is the channel vector for m^{th} frequency bin of user u . $\boldsymbol{\omega}_{u,m}^k \in \mathbb{C}^{N_R}$ is the receive beamforming vector for m^{th} frequency bin of user u at MI index k and it can be optimally calculated as [12]

$$\boldsymbol{\omega}_{u,m}^k = \left(\sum_{l=1}^U P_{l,m} \boldsymbol{\gamma}_{l,m} \boldsymbol{\gamma}_{l,m}^H \bar{\Delta}_{l,k} + \sigma_v^2 \mathbf{I}_{N_R} \right)^{-1} \boldsymbol{\gamma}_{u,m} P_{u,m}^{\frac{1}{2}}. \quad (5)$$

$\bar{\Delta}_{u,k} \in \mathbb{R}$ is the average residual interference of the soft symbol estimates and is given by

$$\bar{\Delta}_{u,k} = \text{avg}\{\mathbf{1}_{N_F} - \check{\mathbf{b}}^u\}, \quad (6)$$

where $\check{\mathbf{b}}^u = [|\tilde{b}_1^u|^2, |\tilde{b}_2^u|^2, \dots, |\tilde{b}_{N_F}^u|^2]^T \in \mathbb{C}^{N_F}$. The soft symbol estimate \tilde{b}_n^u is calculated as

$$\tilde{b}_n^u = E\{b_n^u\} = \sum_{b_i \in \mathfrak{B}} b_i \Pr(b_n^u = b_i), \quad (7)$$

where \mathfrak{B} is the modulation symbol alphabet, and the symbol *a priori* probability can be calculated by

$$\Pr(b_n^u = b_i) = \left(\frac{1}{2}\right)^{N_Q} \prod_{q=1}^{N_Q} (1 - \bar{z}_{i,q} \tanh(\lambda_{n,q}^u/2)), \quad (8)$$

with $\bar{z}_{i,q} = 2z_{i,q} - 1$ and $\mathbf{z}_i = [z_{i,1}, z_{i,2}, \dots, z_{i,N_Q}]^T$ is the binary representation of the symbol b_i , depending on the modulation mapping. $\lambda_{n,q}^u$ is the *a priori* LLR of the bit $c_{n,q}^u$, provided by the decoder of user u . Plugging (3) and (4) into (2), the convergence constraint can be written as [9]

$$\zeta_{u,k} \geq \xi_{u,k}, \forall u = 1, 2, \dots, U, \forall k = 1, 2, \dots, K, \quad (9)$$

where

$$\xi_{u,k} = \frac{(\bar{\sigma}_{u,k})^2}{4 + (\bar{\sigma}_{u,k})^2 \bar{\Delta}_{u,k}} \quad (10)$$

is constant.

4. POWER VARIANCE CONSTRAINT

Instead of considering the instant PAPR, we will derive the expected variance of the transmit power which is not depending on the instantaneous symbol sequence. Because the power variance is derived similarly for all the users, the user index is omitted in this section. Let $\mathbf{G} = \mathbf{F}^{-1} \mathbf{P}^{\frac{1}{2}} \mathbf{F}$. The entry (m, n) of \mathbf{G} is obtained as

$$g_{m,n} = \frac{1}{N_F} \sum_{l=1}^{N_F} \sqrt{P_l} e^{\frac{j2\pi(l-1)(n-m)}{N_F}}. \quad (11)$$

Let s_m be the m^{th} output of the transmitted waveform after the IFFT as depicted in Fig. 1. Assuming $\mathbb{E}\{[b_n]\} = 1$ and $\mathbb{E}\{b_p b_q^*\} = 0$, $\forall p \neq q$, where b_q^* denotes the complex conjugate of b_q , the average of the transmit power can be calculated as

$$\mu = \text{avg}[|s_m|^2] = \frac{1}{N_F} \sum_{m=1}^{N_F} \mathbb{E}\{|s_m|^2\} = \frac{1}{N_F} \sum_{l=1}^{N_F} P_l. \quad (12)$$

The variance of the output power is given by

$$\begin{aligned} \Sigma^2(\mathbf{P}) &= \frac{1}{N_F} \sum_{k=1}^{N_F} (\mathbb{E}[|s_k|^4] - \mu^2) \\ &= \frac{1}{N_F} \sum_{k=1}^{N_F} [2 \left(\sum_{m=1}^{N_F} |g_{k,m}|^2 \right)^2 - \sum_{m=1}^{N_F} |g_{k,m}|^4] - \mu^2. \end{aligned} \quad (13)$$

The first term reduces to

$$\frac{1}{N_F} \sum_{k=1}^{N_F} \left(\sum_{m=1}^{N_F} |g_{k,m}|^2 \right)^2 = \mu^2. \quad (14)$$

The second term can be expressed as a function of power allocation as

$$\begin{aligned} & \frac{1}{N_F} \sum_{k=1}^{N_F} \sum_{m=1}^{N_F} |g_{k,m}|^4 \\ &= \frac{\mu^2}{N_F} + \frac{1}{N_F^3} \sum_{p,q \in \mathcal{S}_1} P_p P_q + \frac{1}{N_F^3} \sum_{p,q,r,s \in \mathcal{S}_2} \sqrt{P_p P_q P_r P_s}, \end{aligned} \quad (15)$$

where $\mathcal{S}_1 = \{p, q \in \{1, 2, \dots, N_F\} : p \neq q, p - q = \pm N_F/2\}$ and $\mathcal{S}_2 = \{p, q, r, s \in \{1, 2, \dots, N_F\} : p \neq q, r \neq s, (p, q) \neq (r, s), s - r \in \{p - q, N_F + p - q, -N_F + p - q\}\}$. Substituting (14) and (15) to (13) we get

$$\begin{aligned} \Sigma^2(\mathbf{P}) &= \frac{N_F - 1}{N_F^3} \left(\sum_{l=1}^{N_F} P_l \right)^2 - \frac{1}{N_F^3} \sum_{p,q \in \mathcal{S}_1} P_p P_q - \\ & \quad \frac{1}{N_F^3} \sum_{p,q,r,s \in \mathcal{S}_2} \sqrt{P_p P_q P_r P_s}. \end{aligned} \quad (16)$$

The objective is to control the variance of the normalized power and hence P_l in (16) is divided by $\sum_{n=1}^{N_F} P_n, \forall l$, resulting in

$$\Sigma^2(\mathbf{P}) \leq \sigma_s^2 \left(\sum_{l=1}^{N_F} P_l \right)^2, \quad (17)$$

where $\sigma_s^2 \in \mathbb{R}^+$ is the maximum variance of the normalized power. Plugging (16) to (17) the constraint can be written as

$$\begin{aligned} (N_F - 1) \left(\sum_{l=1}^{N_F} P_l \right)^2 &\leq \sum_{p,q \in \mathcal{S}_1} P_p P_q + \\ & \sum_{p,q,r,s \in \mathcal{S}_2} \sqrt{P_p P_q P_r P_s} + \left(\sum_{l=1}^{N_F} P_l \right)^2 \sigma_s^2 N_F^3. \end{aligned} \quad (18)$$

5. SUCCESSIVE CONVEX APPROXIMATION

Our objective is to minimize the total transmitted power with the constraints (9) and (18). Hence, the objective is linear but both (9) and (18), are nonconvex constraints. However, we can derive a successive convex approximation for the problem via GP using the inequality [9]

$$\sum_{m=1}^{N_F} t_m \geq \prod_{m=1}^{N_F} \left(\frac{t_m}{\Phi_m} \right)^{\Phi_m}, \quad (21)$$

where $\Phi_m = \frac{\hat{t}_m}{\sum_{n=1}^{N_F} \hat{t}_n}$, $\hat{t}_m > 0$, and $t_m > 0$, $m = 1, 2, \dots, N_F$. Reader should be notified that GP is not convex as such but it can be reformulated as a convex problem [10].

The constraint (9) can be equivalently written as [9]

$$\begin{aligned} & \frac{1}{N_F} \sum_{n=1}^{N_F} t_{u,n}^k \geq \xi_{u,k}, u = 1, 2, \dots, U, k = 1, 2, \dots, K, \\ & P_{u,m} |\boldsymbol{\omega}_{u,m}^k \boldsymbol{\gamma}_{u,m}^H|^2 \geq \\ & \left(\sum_{l=1}^U P_{l,m} |\boldsymbol{\omega}_{u,m}^k \boldsymbol{\gamma}_{l,m}^H|^2 \bar{\Delta}_{l,k} + \|\boldsymbol{\omega}_{u,m}^k\|^2 \sigma_v^2 \right) t_{u,m}^k, \\ & u = 1, 2, \dots, U, \forall k = 1, 2, \dots, K, m = 1, 2, \dots, N_F. \end{aligned} \quad (22)$$

Applying (21) to the first part of (22) yields [9]

$$\begin{aligned} & \prod_{n=1}^{N_F} \left(\frac{t_{u,n}^k}{\Phi_{u,n}^k} \right)^{\Phi_{u,n}^k} \geq N_F \xi_{u,k}, u = 1, 2, \dots, U, k = 1, 2, \dots, K, \\ & P_{u,m} |\boldsymbol{\omega}_{u,m}^k \boldsymbol{\gamma}_{u,m}^H|^2 \geq \\ & \left(\sum_{l=1}^U P_{l,m} |\boldsymbol{\omega}_{u,m}^k \boldsymbol{\gamma}_{l,m}^H|^2 \bar{\Delta}_{l,k} + \sigma_v^2 \|\boldsymbol{\omega}_{u,m}^k\|^2 \right) t_{u,m}^k, \\ & u = 1, 2, \dots, U, k = 1, 2, \dots, K, m = 1, 2, \dots, N_F, \end{aligned} \quad (23)$$

which is a valid GP constraint.

Similarly, applying (21) two times to the RHS of (18) yields a constraint (19) given on the top of next page, where the weights $\tau_u^{(1)}$, $\tau_u^{(2)}$, $\tau_u^{(3)}$ and $\tau_u^{(4)}$ are given in (20) and

$$\begin{aligned} \theta_{u,pq}^{(1)} &= \frac{P_{u,p} P_{u,q}}{\sum_{p',q' \in \mathcal{S}_1} P_{u,p'} P_{u,q'}}, \\ \theta_{u,pqr}^{(2)} &= \frac{\sqrt{P_{u,p} P_{u,q} P_{u,r} P_{u,s}}}{\sum_{p',q',r',s' \in \mathcal{S}_2} \sqrt{P_{u,p'} P_{u,q'} P_{u,r'} P_{u,s'}}}, \\ \theta_{u,l}^{(3)} &= \frac{P_{u,l}^2}{\sum_{l'=1}^{N_F} P_{u,l'}^2}, \theta_{u,l}^{(4)} = \frac{P_{u,p} P_{u,q}}{\sum_{\substack{p',q'=1 \\ q' > p'}}^{N_F} P_{u,p'} P_{u,q'}}. \end{aligned} \quad (24)$$

A successive convex approximation of both the convergence and power variance constrained power minimization problem can be written as

$$\begin{aligned} & \text{minimize} \quad \text{tr}\{\mathbf{P}\} \\ & \text{subject to} \quad \prod_{n=1}^{N_F} \left(\frac{t_{u,n}^k}{\Phi_{u,n}^k} \right)^{\Phi_{u,n}^k} \geq N_F \xi_{u,k}, \\ & \quad u = 1, 2, \dots, U, k = 1, 2, \dots, K, \\ & \quad P_{u,m} |\boldsymbol{\omega}_{u,m}^k \boldsymbol{\gamma}_{u,m}^H|^2 \geq \\ & \quad \left(\sum_{l=1}^U P_{l,m} |\boldsymbol{\omega}_{u,m}^k \boldsymbol{\gamma}_{l,m}^H|^2 \bar{\Delta}_{l,k} + \sigma^2 \|\boldsymbol{\omega}_{u,m}^k\|^2 \right) t_{u,m}^k, \\ & \quad u = 1, 2, \dots, U, k = 1, 2, \dots, K, \\ & \quad m = 1, 2, \dots, N_F, \\ & \quad (N_F - 1) \left(\sum_{l=1}^{N_F} P_{u,l} \right)^2 \leq \mathcal{A}_u(\mathbf{P}_u), u = 1, 2, \dots, U, \\ & \quad P_{u,m} \geq 0, u = 1, 2, \dots, U, m = 1, 2, \dots, N_F, \end{aligned} \quad (25)$$

where $\mathcal{A}_u(\mathbf{P}_u)$ denotes the RHS of (19). The SCA algorithm is summarized in **Algorithm 1**, where the superscript * denotes the optimal solution of (25). Due to the inequality (21), the monomial approximation is never above the approximated summation¹. Hence, **Algorithm 1** is guaranteed to monotonically converge to a locally optimal solution.

Algorithm 1 Successive convex approximation algorithm.

- 1: Set $\hat{t}_{u,n}^k = \hat{t}_{u,n}^{k(0)}, \forall u, k, n$ and $\hat{\mathbf{P}}_{u,n} = \hat{\mathbf{P}}_{u,n}^{(0)}, \forall u, n$.
 - 2: **repeat**
 - 3: Calculate the weights (24) and (20).
 - 4: Solve Eq. (25).
 - 5: Update $\hat{t}_{u,n}^k = t_{u,n}^{k(*)}, \forall u, k, n$ and $\hat{\mathbf{P}}_{u,n} = \hat{\mathbf{P}}_{u,n}^{(*)}, \forall u, n$.
 - 6: **until** Convergence.
-

6. NUMERICAL RESULTS

In this section, numerical results are shown to demonstrate the performance of the proposed algorithm. SCA presented in Section 5

¹By projecting the optimal solution from the approximated problem (25) to the original constraint functions (9) and (18) constraints become loose and thus, the objective can always be reduced.

$$(N_F - 1) \left(\sum_{l=1}^{N_F} P_{u,l} \right)^2 \leq \left(\frac{\prod_{p,q \in \mathcal{S}_1} \left(\frac{P_{u,p} P_{u,q}}{\theta_{u,pq}^{(1)}} \right)^{\theta_{u,pq}^{(1)}}}{\tau_u^{(1)}} \right)^{\tau_u^{(1)}} \left(\frac{\prod_{p,q,r,s \in \mathcal{S}_2} \left(\frac{\sqrt{P_{u,p} P_{u,q} P_{u,r} P_{u,s}}}{\theta_{u,pqrs}^{(2)}} \right)^{\theta_{u,pqrs}^{(2)}}}{\tau_u^{(2)}} \right)^{\tau_u^{(2)}} \\ \times \left(\frac{\sigma_s^2 N_F^3 \prod_{l=1}^{N_F} \left(\frac{P_{u,l}^2}{\theta_{u,l}^{(3)}} \right)^{\theta_{u,l}^{(3)}}}{\tau_u^{(3)}} \right)^{\tau_u^{(3)}} \left(\frac{2\sigma_s^2 N_F^3 \prod_{\substack{p,q=1 \\ q > p}}^{N_F} \left(\frac{P_{u,p} P_{u,q}}{\theta_{u,pq}^{(4)}} \right)^{\theta_{u,pq}^{(4)}}}{\tau_u^{(4)}} \right)^{\tau_u^{(4)}} \quad (19)$$

$$\tau_u^{(1)} = \frac{\sum_{p,q \in \mathcal{S}_1} P_{u,p} P_{u,q}}{\sum_{p,q \in \mathcal{S}_1} P_{u,p} P_{u,q} + \sum_{p,q,r,s \in \mathcal{S}_2} \sqrt{P_{u,p} P_{u,q} P_{u,r} P_{u,s}} + \left(\sum_{l=1}^{N_F} P_{u,l} \right)^2 \sigma_s^2 N_F^3} \\ \tau_u^{(2)} = \frac{\sum_{p,q,r,s \in \mathcal{S}_2} \sqrt{P_{u,p} P_{u,q} P_{u,r} P_{u,s}}}{\sum_{p,q \in \mathcal{S}_1} P_{u,p} P_{u,q} + \sum_{p,q,r,s \in \mathcal{S}_2} \sqrt{P_{u,p} P_{u,q} P_{u,r} P_{u,s}} + \left(\sum_{l=1}^{N_F} P_{u,l} \right)^2 \sigma_s^2 N_F^3} \\ \tau_u^{(3)} = \frac{\sigma_s^2 N_F^3 \sum_{l=1}^{N_F} P_{u,l}^2}{\sum_{p,q \in \mathcal{S}_1} P_{u,p} P_{u,q} + \sum_{p,q,r,s \in \mathcal{S}_2} \sqrt{P_{u,p} P_{u,q} P_{u,r} P_{u,s}} + \left(\sum_{l=1}^{N_F} P_{u,l} \right)^2 \sigma_s^2 N_F^3} \\ \tau_u^{(4)} = \frac{2\sigma_s^2 N_F^3 \sum_{\substack{p,q=1 \\ q > p}}^{N_F} P_{u,p} P_{u,q}}{\sum_{p,q \in \mathcal{S}_1} P_{u,p} P_{u,q} + \sum_{p,q,r,s \in \mathcal{S}_2} \sqrt{P_{u,p} P_{u,q} P_{u,r} P_{u,s}} + \left(\sum_{l=1}^{N_F} P_{u,l} \right)^2 \sigma_s^2 N_F^3}. \quad (20)$$

was derived for fixed receiver. The joint optimum can be achieved via alternating optimization [9] which means that the problem is split to the optimization of transmit power for fixed receiver and optimization of receiver for fixed power allocation. Alternating between these two optimization steps converges to a local solution.

The following parameters is used in simulations: $U = 2$, $N_R = 2$, $N_F = 8^2$, QPSK with Gray mapping, and systematic repeat accumulate (RA) code [13] with a code rate 1/3 and 8 internal iterations are used. The signal-to-noise ratio per receiver antenna averaged over frequency bins is defined by $\text{SNR} = \text{tr}\{\mathbf{P}\} / (N_R N_F \sigma_v^2)$. The channel we consider is a quasi-static Rayleigh fading 5-path average equal gain channel. PAPR is defined as

$$\text{PAPR} = \frac{\max_m |s_m|^2}{\text{avg}[|s_m|^2]}. \quad (26)$$

The complementary cumulative distribution function (CCDF) of PAPR for user 2 for different values of σ_s^2 is depicted in Fig. 2. CCDF is calculated such that 10^5 randomly generated symbol sequences of length N_F for each user is sent over 200 channel realizations. It can be seen from the Fig. 2 that when $\sigma_s^2 = 0.1$ there is not much difference compared to the case where there is no variance constraint. When $\sigma_s^2 = 0.01$ we can obtain a slight PAPR gain with roughly the same SNR compared to the case with no variance constraint. When σ_s^2 is further reduced to 0.001 the PAPR gain is significant. Even though the required SNR to achieve the target MI point increases 1.6 dB, the PAPR gain is much larger than the SNR loss. For example, in the case of no normalized variance constraint we may need to set the maximum transmission power according to 8 dB PAPR while in the case of $\sigma_s^2 = 0.001$ the PAPR corresponding the same value of CCDF ($10^{-4.74}$) is 3.06 dB. Hence, for $10^{-4.74}$ outage the gain is 8 dB - 3.06 dB - 1.6 dB = 3.34 dB. Therefore, the

²The results would be similar with higher N_F . N_F is set rather small to speed up the simulations. In practise, an efficient problem specific solver would be implemented which is fast even with large N_F .

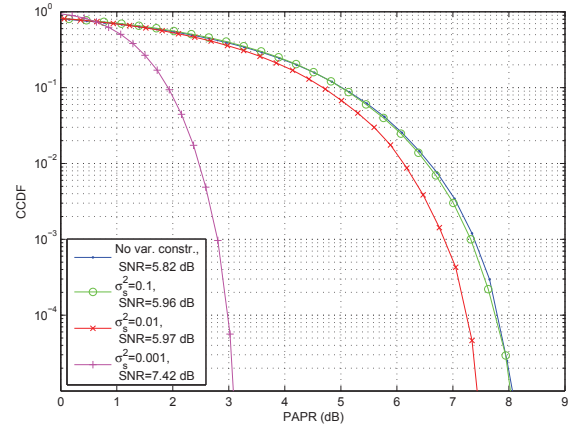


Fig. 2. CCDF of PAPR for user 2. $U = 2$, $N_F = 8$, $N_R = 2$, $\hat{I}_{u,\text{target}}^E = 0.7892$, $u = 1, 2$, $\hat{I}_u^E = 0.9998$, $\forall u$, $\epsilon_u = 0.01$, $\forall u$, $N_L = 5$.

coverage of $\sigma_s^2 = 0.001$ precoded transmission is larger compared to the case with no variance constraint.

7. CONCLUSIONS

Transmission power variance constrained power allocation for iterative frequency domain multiuser single input multiple output detector was derived in this paper. The precoding technique takes into account the convergence properties of the iterative receiver while keeping the transmission power variance below the desired threshold. Successive convex approximation (SCA) approach via series of geometric programs (GP) is developed. Numerical results demonstrated that the PAPR gain is significantly larger than the SNR loss in the variance constrained precoding technique compared to the case without variance constraint. Hence, the proposed precoding technique increases the coverage of the transmission and is beneficial for power limited cell edge users.

8. REFERENCES

- [1] F. Panchaldi, G.M. Vitetta, R. Kalbasi, N. Al-Dhahir, M. Uysal, and H. Mheidat, "Single-carrier frequency domain equalization," *Signal Processing Magazine, IEEE*, vol. 25, no. 5, pp. 37–56, 2008.
- [2] S.B. Slimane, "Reducing the peak-to-average power ratio of ofdm signals through precoding," *Vehicular Technology, IEEE Transactions on*, vol. 56, no. 2, pp. 686–695, 2007.
- [3] D.D. Falconer, "Linear precoding of ofdma signals to minimize their instantaneous power variance," *Communications, IEEE Transactions on*, vol. 59, no. 4, pp. 1154–1162, 2011.
- [4] C.H.G. Yuen and B. Farhang-Boroujeny, "Analysis of the optimum precoder in sc-fdma," *Wireless Communications, IEEE Transactions on*, vol. 11, no. 11, pp. 4096–4107, 2012.
- [5] C. Studer and E.G. Larsson, "Par-aware large-scale multi-user mimo-ofdm downlink," *Selected Areas in Communications, IEEE Journal on*, vol. 31, no. 2, pp. 303–313, 2013.
- [6] J. Karjalainen, M. Codreanu, A. Tölli, M. Juntti, and T. Matsumoto, "EXIT chart-based power allocation for iterative frequency domain MIMO detector," *IEEE Trans. Signal Processing*, vol. 59, no. 4, pp. 1624–1641, Apr. 2011.
- [7] S. ten Brink, "Convergence behavior of iteratively decoded parallel concatenated codes," *IEEE Trans. Commun.*, vol. 49, no. 10, pp. 1727–1737, Oct. 2001.
- [8] V. Tervo, A. Tölli, J. Karjalainen, and T. Matsumoto, "On convergence constraint precoder design for iterative frequency domain multiuser SISO detector," in *Proc. Annual Asilomar Conf. Signals, Syst., Comp.*, Pacific Grove, CA, USA, Nov.4–7 2012, pp. 473–477.
- [9] V. Tervo, A. Tölli, J. Karjalainen, and T. Matsumoto, "Convergence constrained multiuser transmitter-receiver optimization in single carrier FDMA," *IEEE Trans. Signal Processing*, 2013, (under review), arXiv:1310.8067.
- [10] S. Boyd and L. Vandenberghe, *Convex Optimization*, Cambridge Univ. Press, Cambridge, U.K., 2004.
- [11] Mung Chiang, "Nonconvex optimization for communication networks," in *Advances in Applied Mathematics and Global Optimization*, David Y. Gao and Hanif D. Sherali, Eds., vol. 17 of *Advances in Mechanics and Mathematics*, pp. 137–196. Springer US, 2009.
- [12] J. Karjalainen, *Broadband Single Carrier Multi-Antenna Communications with Frequency Domain Turbo Equalization*, Ph.D. thesis, University of Oulu, Oulu, Finland, 2011.
- [13] D. Divsalar, H. Jin, and R. J. McEliece, "Coding theorems for 'turbo-like' codes," in *Proc. Annual Allerton Conf. Commun., Contr., Computing*, Urbana, Illinois, USA, Sept.23–25 1998, pp. 201–210.